JOURNAL GEOLOGICAL SOCIETY OF INDIA
Vol.75, January 2010, pp.18-31

Structural Evolution of a Gneiss Dome in the Axial Zone of the Proterozoic South Delhi Fold Belt in Central Rajasthan

DHRUBA MUKHOPADHYAY[1], NANDINI CHATTOPADHYAY[2] and TAPAS BHATTACHARYYA[1]
[1]Department of Geology, University of Calcutta, 35 Ballygunge Circular Road, Kolkata - 700 019
[2]Department of Geological Sciences, Jadavpur University, Kolkata - 700 032
Email: dhruba_38@yahoo.co.uk

Abstract: The structural geometry of the Anasagar gneiss dome in the axial zone of the South Delhi Fold Belt is controlled by polyphase folding. It is classified as a thrust-related gneiss dome and not as a metamorphic core complex. Four phases of deformation have affected both the gneiss and the enveloping supracrustal rocks. D_2 and D_3 deformations probably represent early and late stages of a progressive deformation episode in a simple shear regime combined with compression. The contact between the gneiss and the supracrustal rocks is a dislocation plane (thrust) with top-to-east sense of movement which is consistent with the vergence of the D_2 folds. The thrust had a ramp-and-flat geometry at depth. At the present level of exposure it is a footwall flat (that is, parallel to the gneissosity in the footwall), but it truncates the bedding of the hanging wall at some places and is parallel at others. The thrusting was probably broadly coeval with the D_2 folds and the thrust plane is locally folded by D_2. D_2 and D_3 folds have similar style and orientation as the first and second phases respectively of major folds in the Delhi Supergroup of the South Delhi Fold Belt and these are mutually correlatable. It is suggested that D_1 may be Pre-Delhi in age. Available geochronological data indicate that the emplacement of the Anasagar gneiss predated the formation of volcanic rocks in the Delhi Supergroup and also predated the main crust forming event in the fold belt. The Anasagar gneiss and its enveloping supracrustal rocks are probably older than the Delhi Supergroup.

Keywords: Anasagar gneiss dome, Polyphase folding, Thrust-related gneiss dome, South Delhi Fold Belt, Rajasthan.

INTRODUCTION

Domal structures cored by metamorphic-plutonic rocks and surrounded by supracrustal rocks, often with lower metamorphic grade, and with a shear zone draping over the metamorphic core, are common in many orogenic belts (Tessiyer and Whitney, 2002). Similar structures were described long ago as mantled gneiss domes by Eskola (1949). Interest in such structures was revived when a belt with many such gneiss domes was mapped in the North American Cordillera (Coney, 1980). It was recognized by the geologists working in the Cordillera that the upper supracrustal rocks are separated by an extensional detachment fault from the underlying gneisses exhibiting a mylonitic fabric, and that normal faults characterize the supracrustal unit (Armstrong, 1982). The term 'metamorphic core complex' was coined for such structures, and in the standard model of their formation the origin was linked to extensional tectonics which attenuated the upper crust by brittle faulting and caused the middle and lower crustal material to rise upwards (Lister and Davis, 1989; Wernicke and Axen, 1988; Yin, 1991). As the study of gneiss domes progressed it was realized that other geological processes may also operate in the formation of gneiss domes. For example, gneiss domes may be associated with diapiric flow caused by density inversion (Ramberg, 1981), or folding in a constrictional strain, or superposed folding (Harris et al. 2002; Yin, 1991), or with thrust duplex development (Dunlap et al. 1997; Makovsky et al. 1999) and development of passive roof thrust (Yin, 2002). Yin (2004) proposed an elaborate classification of gneiss domes based on their geometrical characteristics and formation mechanics. According to him these belong to two fundamentally different classes, fault-unrelated and fault-related. Fault-unrelated domes may be magmatic or non-magmatic and fault-related domes may be detachment-related, thrust-related, strike-slip-related or ductile-shear-zone-related. However, to relate a particular type of gneiss dome to its exact mechanism of formation is often difficult, as illustrated by the vastly different interpretations of a number of well-studied gneiss domes in the Himalayas, the North American Cordillera, the Egyptian Eastern Desert and the Barberton terrain (Fowler and Osman, 2001; Fowler et al. 2007; Fritz et al. 1996; Kisters et al. 2003; Yin, 2004). Yin (2004) remarked that the most challenging task is to differentiate between gneiss domes related to extensional detachment faults and those related to thrusts. Examining the deformational and metamorphic history alone may not provide a unique solution, and other features like spatial distribution of the domes in the orogen, cooling ages, presence or absence of synorogenic basins have to be taken into account.

Here we consider the mechanics of formation of a gneiss dome in the South Delhi Fold Belt (SDFB) on the basis of a detailed structural study of the region. The Anasagar gneiss dome in the SDFB (Heron, 1953; Sinha Roy et al. 1998; Roy and Jakhar, 2002), is exposed in the central part of the northern extremity of the SDFB, in the vicinity of Ajmer (26°27' N : 74°38' E) and it occurs as an elongate rectangular body enveloped by quartzites (Fig.1). South of the Anasagar gneiss dome the gneissic rocks reappear after an unexposed stretch occupied by wind-blown sand and alluvium (Fig.1). Here the gneisses (occasionally referred to as Beawar gneiss) form a long tapering tongue in the median part of the supracrustal belt. Heron (1953) and later workers (Gupta et al. 1995) interpreted this as a thrust wedge of the basement in the SDFB. Though the Anasagar gneiss and the median Beawar gneiss occur along the same linear belt Heron (1953) considered the Anasagar body to be younger and occurring as an anticlinally folded laccolithic intrusion within the Delhi Supergroup.

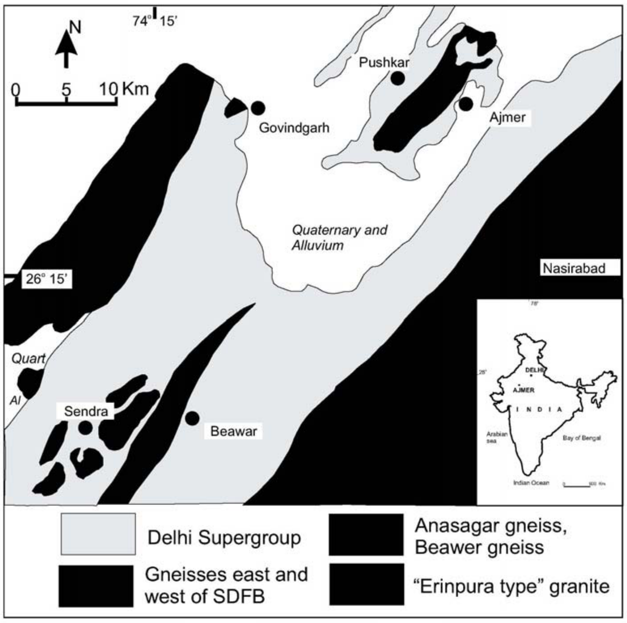

Fig.1. Generalised geological map of the northern part of the South Delhi Fold Belt, adapted from Tobisch et al. (1994) with minor modification.

Fareeduddin et al. (1995), on the contrary, considered the Anasagar gneiss along with its enveloping supracrustals to be older than the stratigraphic units that make up the Delhi Supergroup and tentatively correlated the enveloping supracrustals and the gneiss with the Aravalli Supergroup. They suggested that the Anasagar gneiss can be correlated with the wedge of basement gneiss south of Ajmer (Fig. 1). U-Pb dates of zircons in the Anasagar gneiss suggest a crystallization age of 1849 ± 8 Ma. (Lopez et al. 1996; Mukhopadhyay et al. 2000). Hence it is much older than the time of eruption of acid volcanics in the Delhi Supergroup (zircon U-Pb age: 986.3±2.4 Ma, Deb et al. 2001), the time of crust formation in the SDFB (Sm-Nd age: ~1000 Ma, Volpe and Macdougall, 1990), the time of metamorphic reequilibration in the SDFB (Sm-Nd age: ~800 Ma, Volpe and Macdougall, 1990) or the intrusion of late- to post-tectonic Erinpura Granite batholiths (Rb-Sr age: 730-830 Ma, Chaudhury et al. 1984; ~960 Ma, Tobisch et al. 1994).

GEOLOGICAL SETTING

The supracrustal sequence dominantly made up of quartzite and with minor mica schist, calc-silicate gneiss and amphibolite overlies the Anasagar gneiss (Figs. 2a and b). At several places the quartzite directly overlies the granite gneiss. At other places thin horizons or discontinuous bodies of migmatised mica schist or hornblende-biotite schist or amphibolite occur along the boundary or within the gneiss close to the contact. The gneiss typically contains megacrysts of K-feldspar and is foliated. Magmatic fabric is at places defined by parallel alignment of euhedral megacrysts and alternation of megacryst-rich and megacryst-free bands (Chattopadhyay et al. 2006). The megacrysts are in general recrystallized to aggregates of smaller grains of microcline, often retaining their crystal outline. Post-crystallization deformation has often converted the megacrysts to lensoid augen-like shapes or thin lenticular bands parallel to the foliation or has disrupted them into fragments. Close to the contact, strong deformation has converted the megacrysts into thin elongated streaks (Fig.3a). The structural and textural features indicate that the foliation in the gneiss started as a magmatic structure and subsequently acquired the character of a deformational planar fabric (Chattopadhyay et al. 2006). The floor of the gneiss is not seen anywhere, but in the northern part of the body east of Lohagal, a pelitic/semipelitic schist horizon divides the Anasagar gneiss into two sheets, which merge together in the western part.

The granitic gneiss does not send any discordant tongues

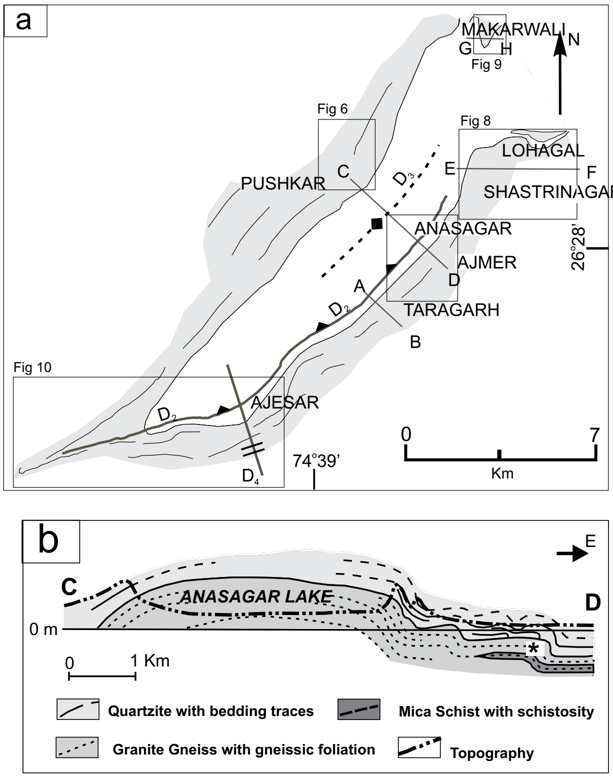

Fig.2. (a) Generalised geological map of Anasagar gneiss and its supracrustal envelope. Trend lines of bedding and axial traces of some major folds are shown. A-B, E-F, G-H are section lines for Fig.7, C-D is section line for Fig.2b. **(b)** Schematic section along C-D, * - Truncation of vertical bedding at horizontal contact surface.

into the overlying supracrustal sequence, but lit par lit injections of quartzofeldspathic veins are present within the mica schists along or close to the contact, and xenoliths of schistose rocks are ubiquitous in the gneiss (Chattopadhyay et al. 2006: Mukhopadhyay et al. 2000). The contact surface is everywhere parallel to the foliation within the gneiss, and at most places it is also parallel to the bedding in the overlying sequence. However, at places subvertical bedding is truncated by subhorizontal contact surface (Fig.2b). Such truncation relation proves that the contact was a plane of dislocation (its significance is discussed later). Along the contact with the supracrustal rocks the gneiss is usually strongly deformed and is converted to finely banded mylonitic gneiss (Fig.3a). The mylonitic foliation is parallel to the main foliation within the body. In addition to this contact zone deformation, mesoscopic shear zones (Fig.3b) of diverse orientation are present throughout the gneiss.

DEFORMATION SEQUENCE

Both the gneiss and the overlying supracrustal rocks are involved in polyphase deformation. Very tight to isoclinal minor folds (Fig.3c) with axial planar schistosity (S_1) are the first phase deformation (D_1) structures in the supracrustal rocks. The sense of vergence of the D_1 folds is generally not decipherable, though at places distinct S and Z shapes are present. The isoclinal folds have not been observed within the granite gneiss or amphibolite, but the gneissic foliation is parallel to the regional schistosity (S_1) in the overlying rocks and is folded by all the later deformation episodes. It is therefore inferred that the emplacement of granite was pre-D_2, and probably syntectonic with D_1, the observed gneissic foliation resulting from a combination of magmatic and deformational (D_1) processes. The mineral and striping lineations in the gneiss and in the metasedimentary rocks are also in part D_1 structures.

The second phase of deformation (D_2) produced asymmetric, large scale, as well as small scale folds. These D_2 folds have alternate gentle-dipping and steep-dipping (occasionally overturned) limbs, with subhorizontal or gentle westerly dipping axial planes (Fig.3d). The D_2 folds have folded the bedding, the bedding-parallel schistosity, and the gneissic foliation. The axial planar fabric is a crenulation cleavage (S_2) which is so intensely developed at certain places that it almost obliterates the earlier schistosity. The axes of D_2 folds are gentle plunging, and are generally coaxial, or have low angles with D_1 fold axes and lineation. The folds are characteristically S-shaped in sectional view looking towards south (Z-shaped looking towards north) (Fig.3d). The consistent easterly vergence of the folds indicates a simple shear regime, with top-to-east sense of movement. It is to be noted, however, that on the short limbs of larger D_2 folds the smaller folds have the expected reversed sense of vergence (Fig.3e). Isoclinal D_1 folds are refolded by D_2 folds (Fig.3f). A particularly instructive exposure in Shastrinagar (about 5 km north of Ajmer) elucidates the relation between the planar fabrics and minor folds of different generations. The exposure lies on the gentle long limb of a major D_2 fold (Fig.4a), and the congruous minor D_2 folds are S-shaped on a vertical section looking to south. An outcrop scale Z-shaped D_1 fold (incongruous with respect to the major D_2 fold) with gentle easterly dipping axial plane is observed in quartz-mica schist with axial planar secondary compositional banding (S_1) (Fig.4b). The shape of the D_1 fold and the angular relation between S_0 (bedding) and S_1 are incongruous with respect to the major D_2 fold. On the limbs of the D_1 fold the S_1 secondary banding (axial planar) is crenulated by D_2 folds having westerly dipping axial planes (Figs. 4c and d).

Upright folds and warps, coaxial with D_2 folds, but with subvertical axial planes, are found on the gentle long limbs

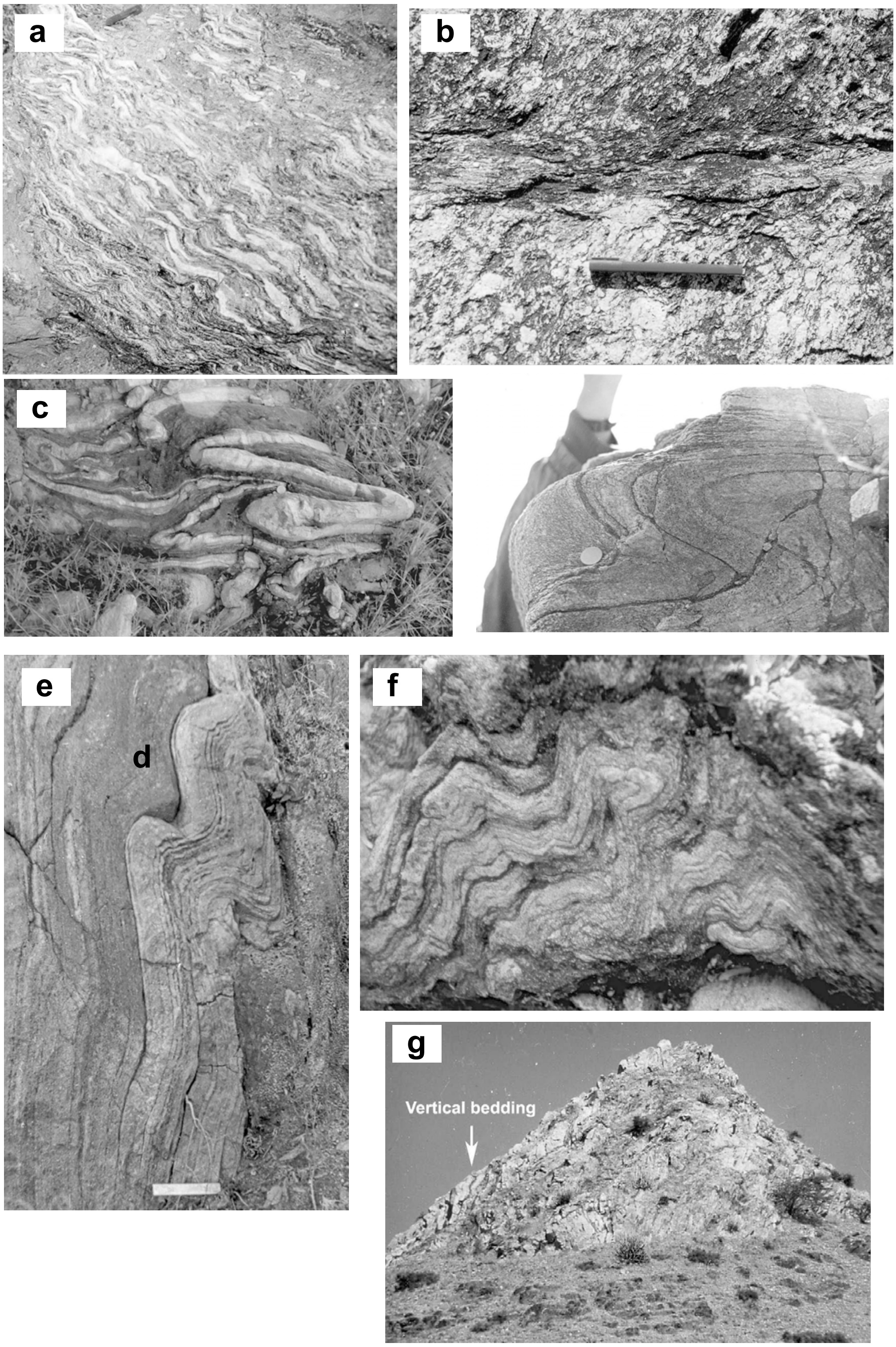

Fig.3. (a) Mylonitic gneiss in the contact zone. Feldspar drawn into streaks and thin bands. Mylonitic banding folded by D_2 crenulations. **(b)** Mesoscopic shear zone with dextral sense of shear in Anasagar gneiss. **(c)** D_1 isoclinal recumbent folds in quartzite interlayered with micaceous bands, on flat limb of D_2 fold. **(d)** D_2 asymmerical folds (S-shaped) with easterly vergence, gentle westerly dipping axial plane. Section looking towards south. **(e)** Z-shaped D_2 folds on steep limb of larger D_2 fold, moderate westerly dipping axial plane. Section looking towards south. **(f)** D_1 isoclinal fold refolded by D_2 folds with steep westerly dipping axial planes; section looking towards south. **(g)** Vertical bedding in quartzite near Makarwali truncated by horizontal contact with underlying granite gneiss (lower part of the photograph). Foliation in gneiss is subhorizontal.

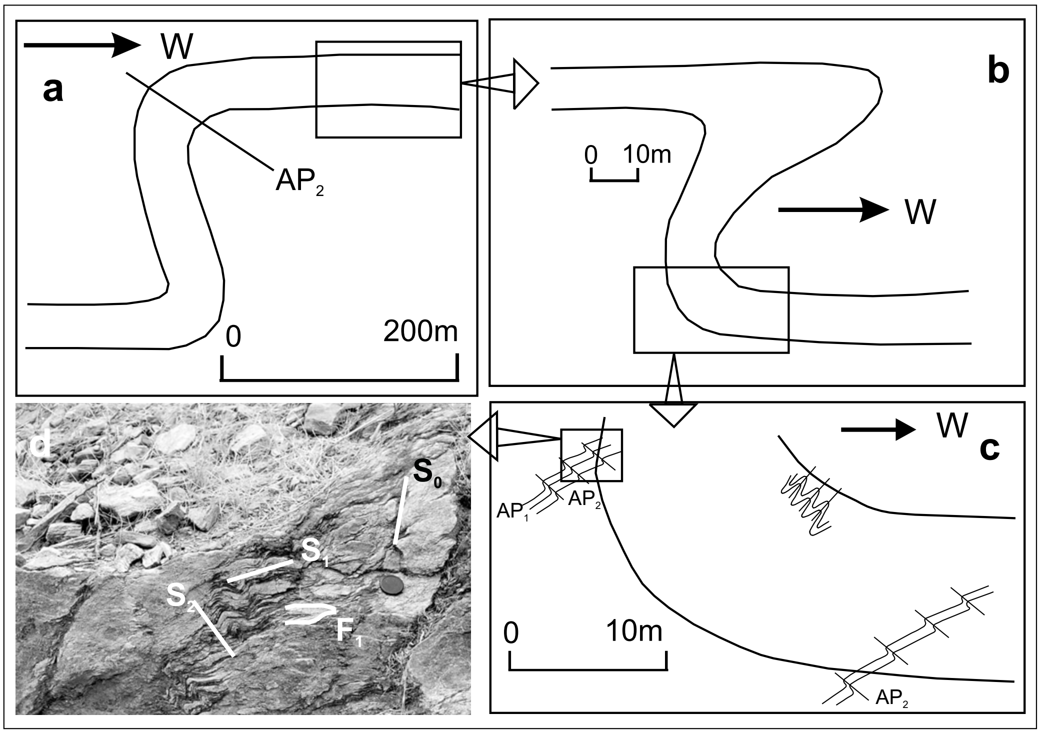

Fig.4. (a, b, c) Schematic representations showing relation between D_1 and D_2 folds and planar fabrics near Shastrinagar. Sections looking towards south. **(d)** Steep limb of D_1 minor fold (top left corner of Fig.9c). Bedding (S_0) with steep easterly dip, D_1 secondary banding (S_1) gentle dipping towards east, D_2 crenulations with axial plane steep dipping towards west. Section looking towards south.

of the D_2 folds. These folds are assigned to a third phase (D_3) of deformation. Examples of such folds bending the D_2 crenulation cleavage are rarely seen (Fig.5). However, in several outcrops, large variation in the dips of the axial planes of neighbouring folds from subhorizontal to steep is observed. Hence it is possible that D_2 and D_3 represent the early and late stages of the same episode of deformation, in a regime with combined shortening and simple shear, the variation in dip of axial planes being produced by progressive rotation of axial plane during simple shear (Mukhopadhyay et al. 1997).

Fig.5. Photomicrograph of D_2 crenulation cleavage bent by D_3 fold.

Superposition of folds (D_4) with transverse (E-W to WNW-ESE) axial planes is evident in the bending of one set of puckers (D_2/D_3) by a later set. D_4 pucker axes are seen to curve around hinge areas of D_2 asymmetric folds. The effects of this last phase of deformation are only sporadically seen.

PATTERN OF MAJOR STRUCTURES

The Anasagar gneiss occupies the core of a D_3 antiformal arch. Detailed structural mapping has brought out the complexities of the overall structural pattern. On the eastern flank of the arch a number of major D_2 folds are mapped and the large D_3 antiformal arch is developed on the flat limb of a D_2 antiformal fold (Fig.2b).

Western Flank of Gneiss Dome

On the western flank of the Anasagar antiformal arch the bedding in quartzite, schistosity in mica schist, and the gneissic foliation in the gneiss all have westerly dip, the amount varying from gentle to steep. The map of a sector on the western flank is shown in Fig.6. The overall dip is gentle here, but in other parts of the western flank the bedding has steep westerly to subvertical dips. No major fold has

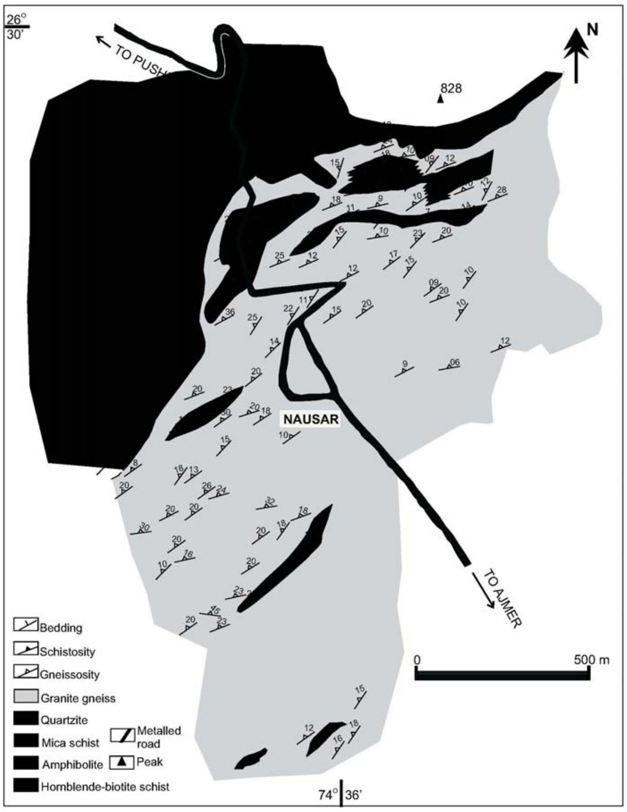

Fig.6. Geological sketch map of a sector on the western flank of Anasagar gneiss.

been observed on the western flank of the arch, but D_2 minor folds are S-shaped looking to south indicating top to east sense of movement.

Eastern Flank of Gneiss Dome

On the eastern flank a number of major folds are observed and detailed structural studies are carried out in the northern part (north of Taragarh, see Fig. 2a for location). Near Taragarh ridge a number of step-like D_2 folds with westerly dipping axial planes and gentle southerly plunge are present (Fig.7a). The steep limbs have moderate easterly dip or are vertical to overturned with steep westerly dip. The main Taragarh ridge represents a steep to moderate easterly dipping limb. There are outcrop scale D_1 folds with gentle to moderate easterly dipping axial planes which are schematically shown in Fig.7a. In contrast, the D_2 minor folds have westerly dipping axial planes, and consequently the D_1 and D_2 folds have at places opposite sense of vergence (Fig.7a inset). The granite gneiss immediately flanking it shows moderate easterly dip and it becomes gentle further west forming the flat limb. The axial trace of this D_2 antiform passes close to the gneiss-supracrustal contact (Fig.2a). Southwards the eastern limb of this fold is overturned and becomes westerly dipping. The flat limb of this fold is antiformally arched by D_3 and the contact is repeated on the western flank (Fig.2b).

A similar structural pattern with a series of major asymmetrical D_2 folds with gentle southerly plunge is also mapped north of Ajmer in the Shastrinagar-Lohagal area (Figs. 8, 7b). Near Lohagal a steep-dipping limb in the supracrustal sequence is truncated by the subhorizontal gneiss-supracrustal contact; the underlying gneiss has gneissic foliation parallel to the contact. Further east the bedding again becomes parallel to the contact and to the gneissic foliation in the underlying rocks (Fig.7b). The truncation points to the existence of a dislocation along the contact. The strong deformation along the contact has turned the megacryst-bearing gneiss to a finely banded rock in which the megacrysts are drawn out to long, thin lenticular streaks (Fig.3a).

The flat land north of Lohagal is occupied by the granite gneiss underlying the mica schist. Further north, as a result of plunge reversal the mica schist and the overlying quartzite are again exposed near Makarwali and form small hillocks (Fig.9). The bedding in the overlying quartzite is folded into asymmetrical, gentle northerly plunging D_2 folds, the steep limbs of which are truncated by the subhorizontal contact (Figs.3g, 7c, 9). Movement along the contact has dragged the subvertical bedding into a subhorizontal attitude parallel to the contact, the sense of drag indicating top-to-east sense of movement (Fig.7c inset), consistent with the sense of vergence of the D_2 folds. The westernmost subhorizontal limb of D_2 folds is folded by a D_3 synform with subvertical axial plane (Fig. 7c).

Southern Closure of Gneiss Dome

In the northern sectors the folds of different generations are gentle plunging, and structurally the gneiss underlies the supracrustal rocks, the stratigraphic younging direction in quartzite being away from the gneiss (Mukhopadhyay et al. 2000). At the southern closure of the gneiss dome the strike of the bedding in the quartzite swings to E-W direction, but the dip is steep towards north, so that the granite appears to structurally overlie the quartzite (Fig.10). This southern closure represents the bent overturned limb of the westernmost D_2 antiform mapped west of Taragarh, the bending being caused by a D_4 fold (Figs. 2a, 10). It is not the closure of a D_2 or D_3 antiformal arch. The axial trace of the D_2 fold is bent by the D_4 fold and the D_2 hinge is exposed as an acute V-shaped closure in the southwestern corner of the Anasagar dome (Figs.2a and 10). Therefore it is concluded that the southern U-shaped broad closure does not represent the hinge zone of the gentle plunging D_3 as surmised by Heron (1953).

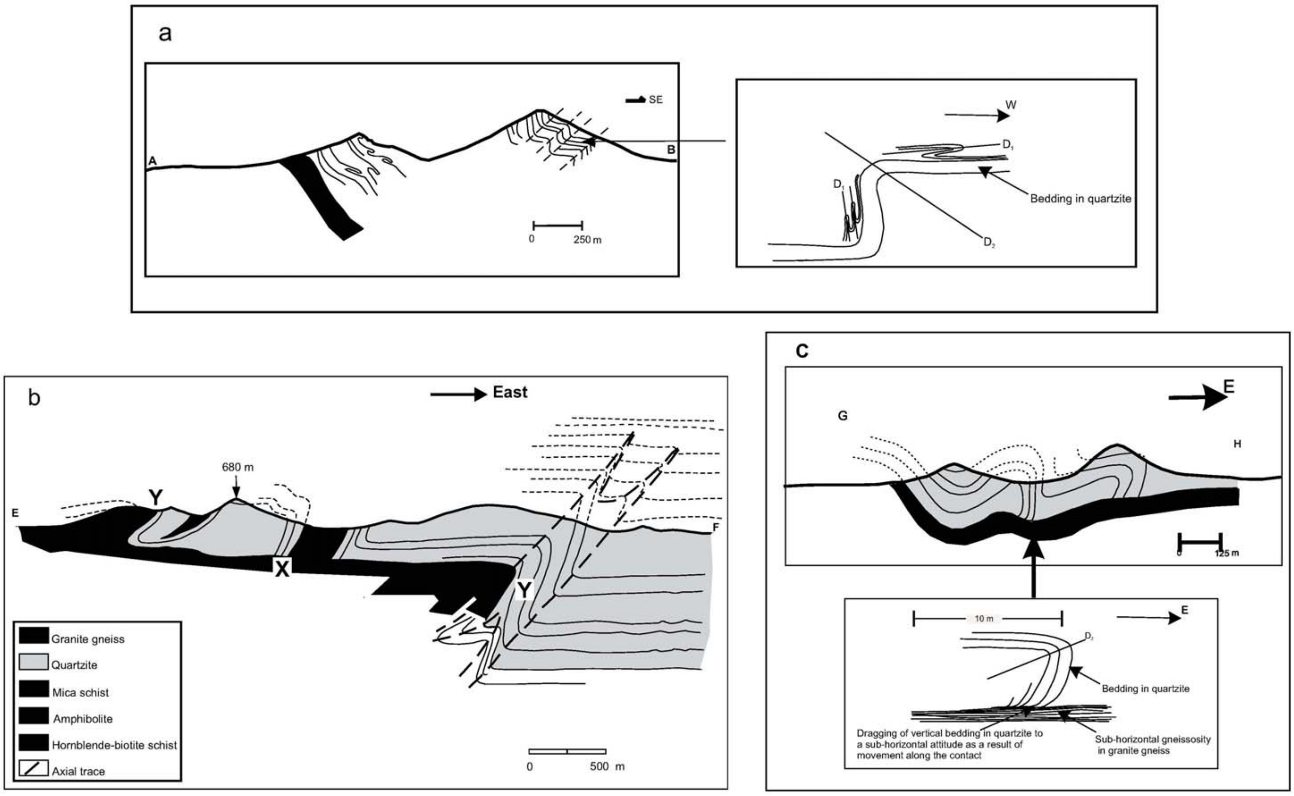

Fig.7. **(a)** Section across A—B in Fig.2a (Taragarh ridge). Inset — Opposite sense of vergence of D_1 and D_2 folds. **(b)** Cross section across E—F in Figs.2a and 8 (Shastrinagar-Lohagal area). Depth projection is on the basis of plunge of fold axis. X – Truncation of vertical bedding at contact, Y – Bedding parallel to contact. **(c)** Section across G-H in Figs.2a and 9 (Makarwali area). Inset – Drag of vertical bedding in overlying quartzite along contact with gneiss.

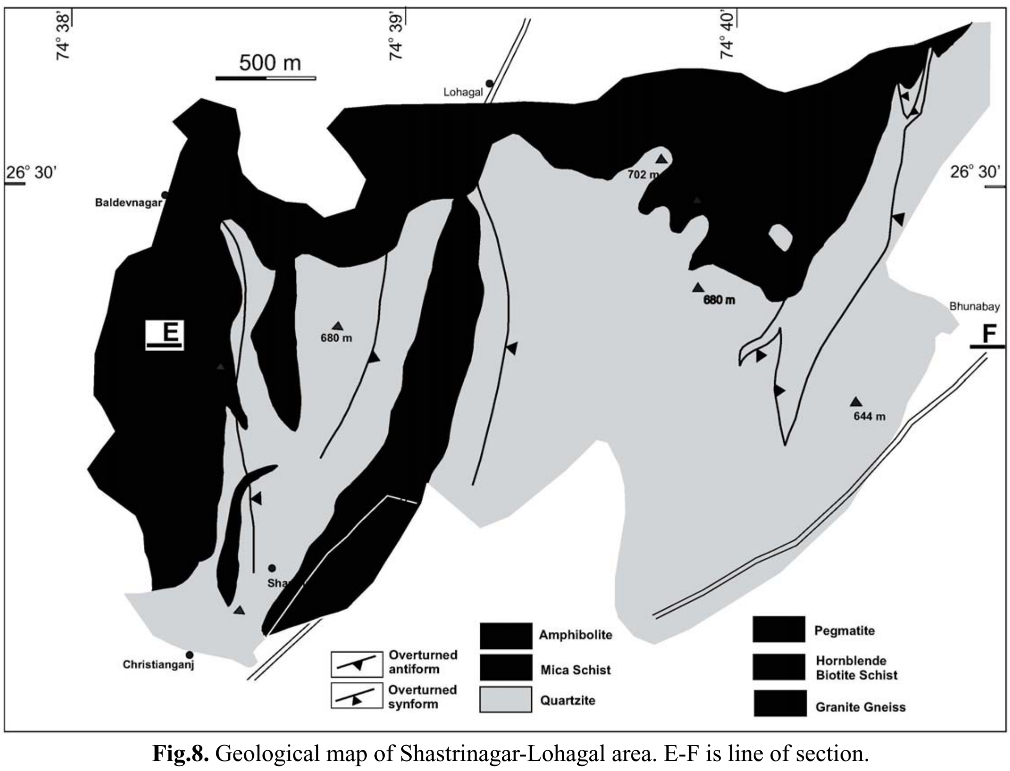

Fig.8. Geological map of Shastrinagar-Lohagal area. E-F is line of section.

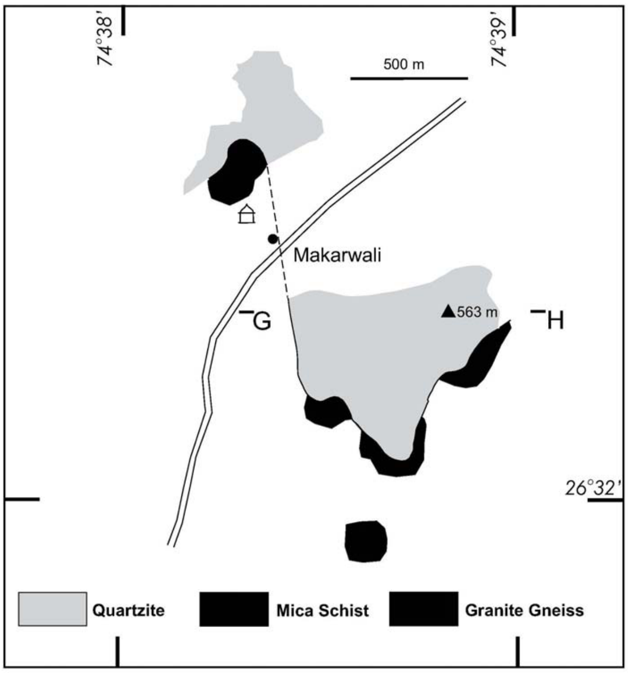

Fig.9. Geological map of Makarwali area. G-H is line of section.

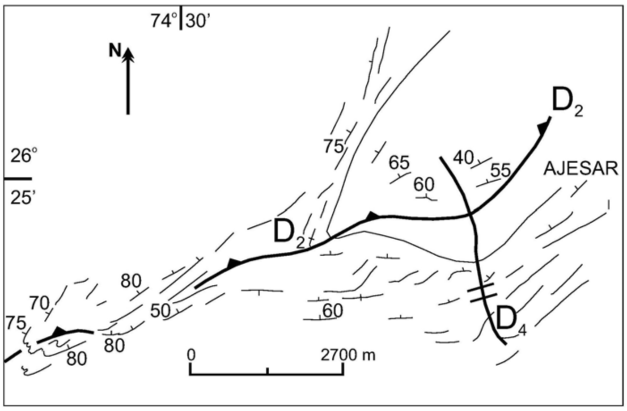

Fig.10. Geological map of southern closure of gneiss dome. Trend lines of bedding and gneissosity with generalized dips and axial traces of D_2 and D_4 folds are shown.

RELATION BETWEEN THE GNEISS AND THE SUPRACRUSTAL SEQUENCE

The intrusive nature of the Anasagar gneiss is indicated by the presence of xenoliths of schistose rocks and rarely of quartzite. On both the eastern and western flanks of the Anasagar gneiss close to the contact the mica schist is migmatised showing lit-per-lit injection of quartzo-feldspathic veins. D_1 isoclinal folds are not present in the gneiss, but the gneissic foliation is parallel to the D_1 axial planar schistosity in the supracrustal rocks. D_2 and D_3 folds have affected the bedding and schistosity in the supracrustal sequence as well as the gneissic foliation in the gneiss. Hence it is concluded that the emplacement of the gneiss is earlier than D_2 and probably syntectonic with D_1. The contact between the gneiss and the supracrustals is a plane of dislocation which is everywhere parallel to the underlying gneissosity; it is at places parallel to bedding in the overlying rocks and folded by the D_2 folds, and at other places it truncates the steep limb in the supracrustal rocks (Figs. 3g, 7b, c). This movement along the contact must have been broadly coeval with the D_2 folding because though at places it truncates the steep limb, at other places it is folded by the D_2 folds. Furthermore, the top-to-east sense of movement on the dislocation is consistent with the easterly vergence of the D_2 folds.

Ductile deformation in the gneiss along the contact has converted it to banded mylonitic rock. On the mylonitic foliation the stretching lineation is mostly subhorizontal with N-S trend, parallel to the regional fold axis. Several textural features, such as, asymmetric tails of porphyroclasts, bookshelf sliding, C' shear bands suggestive of shear movement along the foliation surface in the gneiss are commonly observed (Fig.11 in Chattopadhyay et al. 2006). The sense of movement deduced from these conform with top-to-east sense of movement. Small scale shear zones cutting across the gneissosity are sporadically seen (Fig. 3b). Within these the gneiss is transformed to a finely foliated quartzo-fedspathic schist with foliation parallel to the shear zone walls. Both dextral and sinistral sense of shear are observed in such shear zones. The temporal relation of these shear zones with the folding episodes is ambiguous.

ORIENTATION PATTERNS OF PLANAR AND LINEAR FABRICS

The geometrical patterns of planar and linear fabrics have been analysed by subdividing the whole area into four sectors (Taragarh, Shastrinagar, east of Lohagal and Makarwali, Fig.2a) and plotting the structural data in lower hemisphere equal area projection diagrams. The data are given in Table 1 and representative equal area plots are shown in Fig.11. The modal orientations of planes and lines and the poles to the best-fit great circles are determined by computing the eigen vectors (Woodcock, 1977). Cones of confidence (95% level) are determined by usual statistical techniques, assuming Bingham distribution.

Bedding in quartzite, gneissic foliation in granite gneiss and schistosity in mica schist are subparallel (Table 1) and show very similar great circle patterns caused by the presence of large D_2 and D_3 folds (Figs.11a-j). Deviations from an ideal great circle (e.g. Figs. 11a, d, f) are due to D_4 warps. The calculated great circle pole (β) represents the axis of

Table 1. Summary of orientation data

TARAGARH

Rock Type	Structural Elements	Fig.	N	Representative Attitude: Pole to Great Circle	Modal Orientation of Line	Modal orientation of Plane	Semi-Apical Angle of Cone of Confidence: Measured With	Plane of measurement: $\lambda_1 - \lambda_2$	$\lambda_2 - \lambda_3$	$\lambda_1 - \lambda_3$
QUARTZITE	Pole to Bedding and Schistosity	11a	199			017/44	λ_1	3.87		4.1
				12→185			λ_3		11.89	4.1
	D2 and D3 Axes	11k	35		18→193		λ_1	9.95		11.42
	Pole to D2 Ax. Pl.		10	1→204			λ_3		14.26	11.71
	Pole to D3 Ax. Pl.		13			002/82				
	Pole to D1 Ax. Pl.		3							
	Lineation		33							
GNEISS	Pole to Foliation	11b	100			024/37	λ_1	3.32		3.44
	D2 Axes		15		22→170		λ_1	17.28		22.22
	Pole to D2 Ax. Pl.	11q	11	6→229		212/19	λ_3		35.15	11.2
	Lineation	11w	58		29→134		λ_1	3.56		3.62
MICA SCHIST	Pole to Schist.	11c	70			030/45	λ_1	3.68		3.88
	D2 Axes		10							
	D3 Axes		16		3→33		λ_1	10.86		10.91
	D2 and D3 axes		13		26→181		λ_1	13.21		13.73
	Pole to D2 Ax. Pl.		10							
	Pole to D3 Ax. Pl.		15			208/88	λ_1	9.41		9.56
	Lineation		19		44→140		λ_1	12.23		13.44

EAST OF LOHAGAL

Rock Type	Structural Elements	Fig.	N	Pole to Great Circle	Modal Orientation of Line	Modal orientation of Plane	Semi-Apical Angle of Cone of Confidence: Measured with	Plane of measurement: $\lambda_1 - \lambda_2$	$\lambda_2 - \lambda_3$	$\lambda_1 - \lambda_3$
QUARTZITE	Pole to Bed,/Sch.	11f	678	9→207		139/10	λ_3		2.82	2.14
	D2 Axes		59		19→206		λ_1	3.38		3.55
	D3 Axes		7							
	D2 and D3 Axes		43		13→193		λ_1	4.78		5.28
	Pole to D2 Ax. Pl.	11s	45			195/27	λ_1	4.19		4.24
	Pole to D3 Ax. Pl.	11v	20			199/87	λ_1	8.97		9.04
	Lineation		41		6→192		λ_1	8.01		8.68
GNEISS	Pole to Foliation	11g	215	14→207			λ_3		5.28	2.21
						102/14	λ_1	2.04		2.21
	D2 Axes		36		12→197		λ_1	3.42		3.58
	D2 and D3 Axes		25		18→183		λ_1	4.58		4.8
	Pole to D2 Ax. Pl.		39			189/26	λ_1	5.88		5.97
	Lineation	11z	21		15→184		λ_1	4.35		4.51
SCHIST	Pole to Schistosity	11h	151			115/16	λ_1	1.66		1.78
	D2 Axes		9							
	D2 and D3 Axes		50		14→171		λ_1	2.71		2.77
	Pole to D2 Ax. Pl.		9		86→117		λ_1	14.32		14.95

SHASTRINAGAR

Rock type	Structural Elements	Fig.	N	Representative Attitude: Pole to Great Circle	Modal Orientation of Line	Modal Orientation of Plane	Semi-Apical Angle of Cone of Confidence: Measured with	Plane of measurement: $\lambda_1 - \lambda_2$	$\lambda_2 - \lambda_3$	$\lambda_1 - \lambda_3$
QUARTZITE	Pole to Bed./Sch	11d	897	22→198		146/28	λ_3		1.98	1.8
	D1 Axes	11l	18		18→193		λ_1	5.87		6.05
	D2 Axes	11m	52		20→184		λ_1	4.42		4.54
	D3 Axes	11n	40		23→185		λ_1	4.4		4.54
	D2 and D3 Axes.		42		19→168		λ_1	5.99		6.28
	Pole to D1 Ax.Pl.		13	12→206			λ_3		12.7	13.14
	Pole to D2 Ax.Pl.	11r	56			168/33	λ_1	3.85		4.07
	Pole to D3 Ax.Pl.	11u	47			180/73	λ_1	5.38		5.34
	Pole to D4 Ax.Pl.		3							
	Lineation	11x	353		21→183		λ_1	2.1		2.17
GNEISS	Pole to Foliation	11e	299			57/17	λ_1	1.49		1.53
				15→175			λ_3		6.08	1.53
	D2 Axes		9		19→204		λ_1	8.82		9.01
	D3 Axes		8							
	D2 and D3 Axes		28		21→172		λ_1	4.82		5.26
	Pole to D2 Ax.Pl.		7				λ_1	15.64		16.74
	Pole to D3 Ax.Pl.		4				λ_1	10.89		11.47
	Lineation	11y	252		16→166		λ_1	1.44		1.47

MAKARWALI

Rock type	Structural Elements	Fig.	N	Pole to Great Circle	Modal Orientation of Line	Modal Orientation of Plane	Semi-Apical Angle of Cone of Confidence: Meaured with	Plane of measurement: $\lambda_1 - \lambda_2$	$\lambda_2 - \lambda_3$	$\lambda_1 - \lambda_3$
QUARTZITE	Pole to Bed./Sch	11i	390	29→345			λ_3		2.09	2.22
	D2 Axes	11o	11		27→344		λ_1	7.13		7.44
	D3 Axes	11p	7		29→339		λ_1	5.64		5.8
	D2 and D3 Axes		16		30→346		λ_1	6.93		7.06
	Pole to D2 Ax. Pl.	11t	80			211/32	λ_1	2.87		2.98
	Pole to D3 Ax. Pl.		8			177/79	λ_1	6.96		7.1
	Lineation	11z*	98		28→340		λ_1	2.33		2.39
GNEISS	Pole to Foliation	11j	69			228/29	λ_1	2.16		2.19
	D2 and D3 Axes		9		25→342		λ_1	6.5		6.94
	Pole to D2 Ax. Pl.		3							
	Lineation		14		21→341		λ_1	4.46		4.68
SCH.	Pole to Schistosity		7			219/31	λ_1	7.49		7.51
	Lineation		2							

Dip direction is clockwise from strike direction.

Because of near-coaxiality D2 and D3 Axes cannot always be differentiated. These are plotted together in separate diagrams.

λ_1, λ_2, λ_3 are eigen vectors.

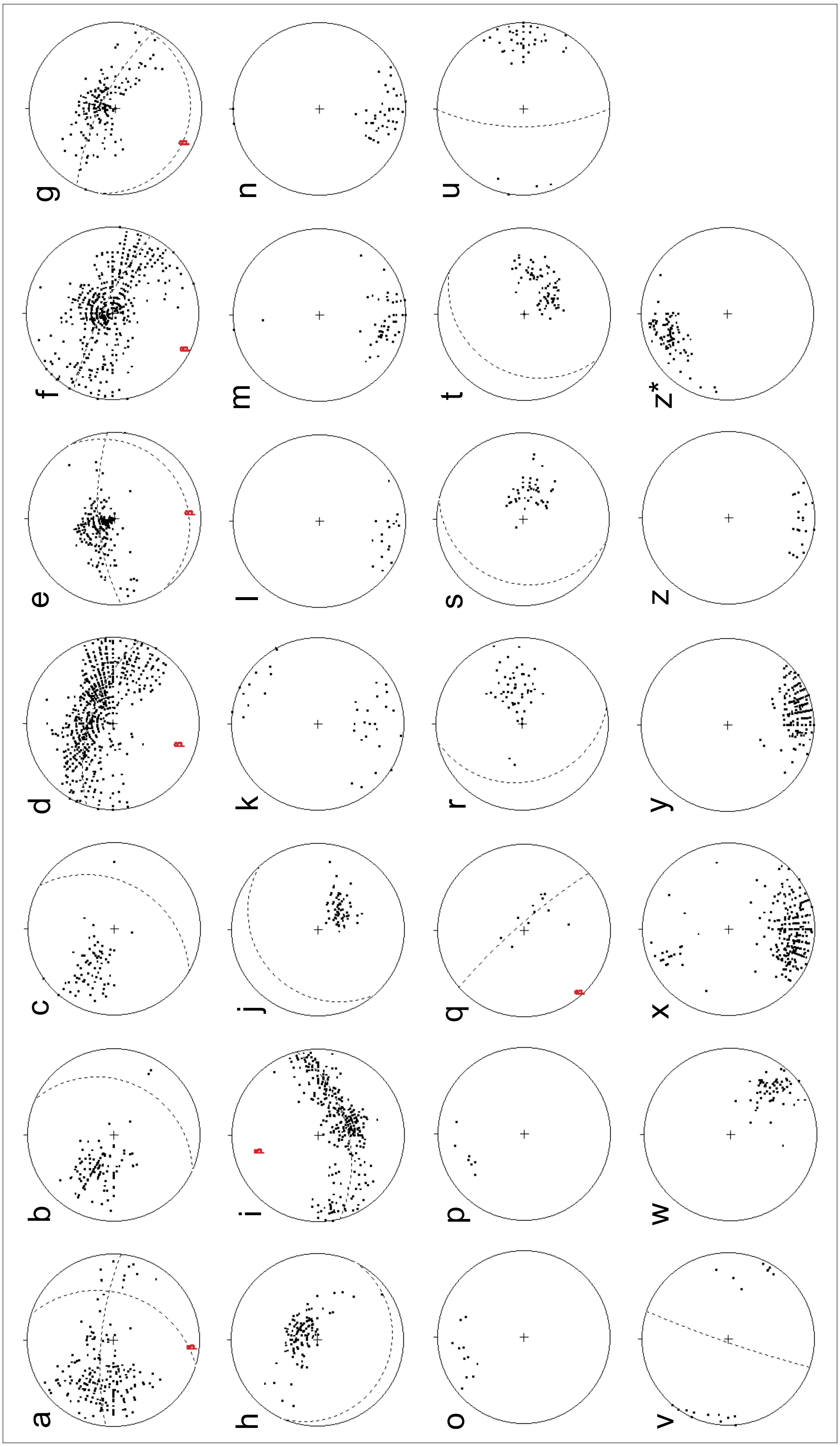

Fig.11. Lower hemisphere equal area projection diagrams of structural data. **(a-j)** Poles to bedding, schistosity, foliation. **(k-p)** D_1-D_2-D_3 fold axes. **(q-t)** Poles to D_2 axial planes. **(u,v)** Poles to D_3 axial planes. **(w-z*)** Lineations. Details in Table 1.

the major coaxial D_2-D_3 folds. A slight difference in the orientations of β in quartzite and in granite gneiss is noticeable in some sectors (Figs.11e, f). This is possibly due to slight discordance in the pre-D_2 orientations of bedding and gneissic foliation. The attitudes of β clearly reveal a regional plunge culmination between Shastrinagar-Lohagal and Makarwali (Figs.11d, f, i). Thus the point of culmination is not at the central part of the gneiss dome but in the northern sector.

D_2 and D_3 minor folds are nearly coaxial and the fold axes are either parallel to or close to the calculated β of the corresponding sector (Figs.11k-o). Deviation from strict parallelism of β and minor fold axes maxima (Figs.11d, l, m) reflects slight non-parallelism of axes of folds on different scales, β representing the axis of the larger folds. Like β, the minor fold axes show gentle southerly plunge in the Taragarh and Shastrinagar-Lohagal sectors, while at Makarwali these are gentle northerly plunging, indicating a regional plunge culmination. The axial planes of D_2 minor folds have gentle to moderate dip (Figs.11p-s) and the axial planes of D_3 folds have N-S to NNE-SSW strike and very steep dip (Figs.11t, u).

The axes of D_1 minor folds are subparallel to axes of D_2 and D_3 folds (Fig.11v), but the axial planes of the former are bent by D_2 and D_3 folds.

In quartzite and mica schist a lineation is defined on the bedding/schistosity (S_1) surface by parallel orientation of elongated mica flakes or elongated micaceous streaks. Elongated streaks of feldspathic material or biotitic streaks define a lineation on the gneissosity surface of the gneiss (Fig.12a). It is best developed in the mylonitic contact zone where it represents the stretching direction during D_2 because the movement is broadly coeval with D_2. Within the gneiss body, however, in the coarser grained gneiss this lineation on the D_1 gneissosity probably defines the stretching direction during D_1 deformation. In the contact zone near Lohagal the lineation is gently plunging subparallel to the D_2 fold axes, but in the Taragarh region steeper plunges oblique to the fold axes are observed. Very rarely the lineation is bent by the D_2 folds (Fig.12b). In the different sectors the lineation maximum (Figs.11w - z*) has a broadly similar, but not identical, orientation as β and D_2-D_3 fold axes maxima in the corresponding sector, the lineation trend being more easterly than those of β or D_2-D_3 maxima. In the Taragarh region the angle between the lineation maximum and the D_2-D_3 maximum is ~40°, while the angle is smaller (~10°) in the Shastrinagar-Lohagal sectors (Table 1). The orientation pattern suggests that the stretching direction during D_1 was at moderate angle to the gently plunging fold axes, but during D_2 the stretching was subparallel to the fold axes. A slight difference (~15°) between the lineation orientations in quartzite and granite gneiss is also noticed in some sectors (Figs.11x, y), indicating that in multilayers the principal axes of strain are not strictly parallel in layers of different rheology.

DISCUSSION

In contrast to the metamorphic core complexes in North American Cordillera there is no evidence that the Anasagar gneiss dome formed in an extensional regime. No normal faults or synorogenic basins (Yin, 2004) associated with normal faulting could be identified. The structural setting

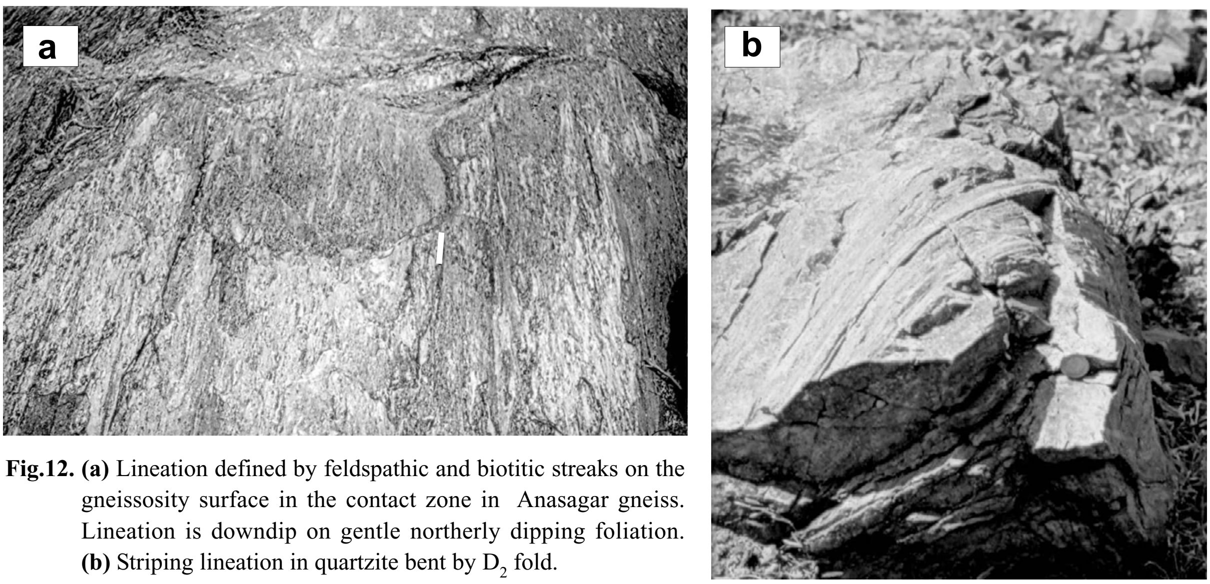

Fig.12. (a) Lineation defined by feldspathic and biotitic streaks on the gneissosity surface in the contact zone in Anasagar gneiss. Lineation is downdip on gentle northerly dipping foliation. **(b)** Striping lineation in quartzite bent by D_2 fold.

suggests its formation in a compressional regime. On the basis of the structural studies the Anasagar gneiss dome may be characterized as a thrust-related dome and its mechanism of formation is related to fault-bend folding associated thrusting (Yin, 2004). Precise estimation of P-T conditions, determination of the cooling ages and thermal modeling could place further constraints on the mechanism of formation of the dome.

The overall geometrical form of the gneiss dome is a result of the interference of D_2, D_3 and D_4 major folds. The dislocation zone along the gneiss-supracrustal contact is everywhere parallel to the foliation in the underlying gneiss and is parallel to the overlying bedding at some places and truncates it at others. This feature suggests that the dislocation zone had a ramp-and-flat geometry. At the present level of exposure it is a flat with respect to the footwall, and the truncations in the upper unit represent hanging wall ramps, and the parallel parts represent hanging wall flats. The ramps and flats on the fault surface are inferred to be located at depth (Fig.13, Stage 1). The easterly vergence of the D_2 folds and the sense of drag at the truncation zones indicate top-to-east sense of movement. As discussed earlier the movement was broadly coeval with D_2 folding or at the early stage of D_2 folding. At the initial stage of movement fault-bend folds were produced (Fig.13, Stage 2). Continued deformation produced the asymmetric and upright folds, which folded the fault plane also (Fig. 13, Stage 3). Subhorizontal fold axis parallel to the D_2 stretching direction is suggestive of deformation in a constrictive regime with maximum elongation in the horizontal direction (Martinez-Martinez et al. 2002; Whitney et al. 2004 and references therein; Yin, 2002). The prolate shapes of pebbles in sporadically occurring pebbly quartzite, and prolate shapes of recrystallized feldspathic pods found at several places close to the contact corroborate this.

The entire rock package had gone through a phase of deformation and granite emplacement before they were folded and faulted by the D_2 and D_3 events. From the limited geochronological data available (summarized earlier) it appears that a time span of nearly 900 Ma separated the D_1 and D_2 events. Furthermore, the style of D_2 and D_3 folds and the easterly vergence of D_2 in Anasagar area are similar to the style of first and second phases of folds respectively in the Delhi Supergroup of the SDFB (Mukhopadhyay, 1989: Mukhopadhyay and Bhattacharyya, 2000). The orientations of their axes and axial planes are also similar. It is, therefore likely that the Anasagar gneiss and its

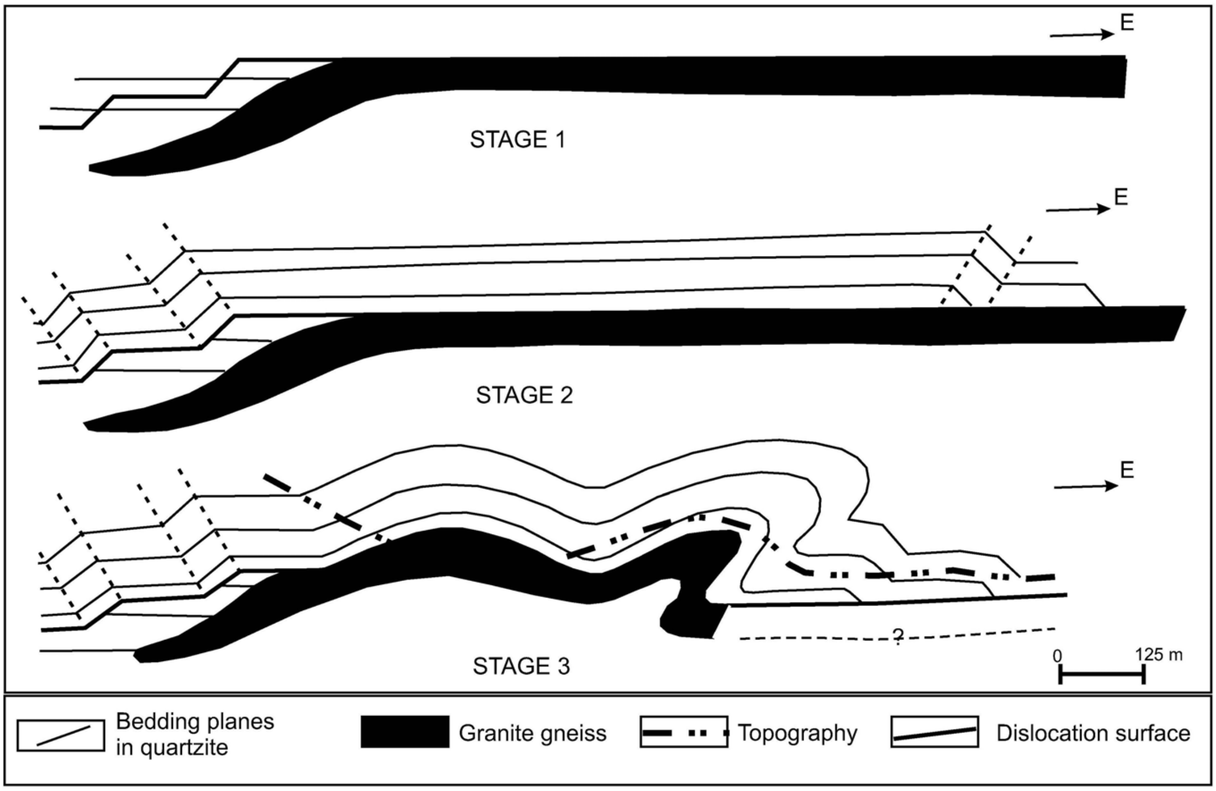

Fig.13. Evolution of structural pattern at different stages of easterly movement of the overlying block on a thrust with ramp-and-flat geometry.

enveloping supracrustal rocks form a part of the Pre-Delhi basement (?Aravalli Supergroup) caught up in the Delhi deformation. These record a Pre-Delhi deformation event (D_1) as well as the events of the Delhi orogeny (D_2 and D_3). The geometrical form as we see it now is a result of polyphase folding during the Delhi orogeny.

Acknowledgements: A major part of the work was done in a research project funded by the Department of Science and Technology, Government of India. DM acknowledges the financial support from the Indian National Science Academy through its Senior Scientist Scheme. We have been benefited by stimulating discussions with Dr. Pratip Gupta. Constructive suggestions from Professors O.T. Tobisch and M.A. Mamtani have improved the manuscript. We are grateful to the Secretary and staff of the Bengali Hindu Dharmashala of Ajmer for help and cooperation during field work.

References

Armstrong, R.L. (1982) Cordilleran metamorphic core complexes - from Arizona to southern Canada. Ann. Rev. Earth Planet. Sci., v.10, pp.129-154

Chattopadhyay, N., Mukhopadhyay, D. and Bhattacharyya, T. (2006) Primary and secondary features in the Anasagar gneiss near Ajmer and their implication on the evolution of the Proterozoic South Delhi Fold Belt, Central Rajasthan. Indian Minerals, v.60, pp.105-118.

Choudhary, A. K., Gopalan, K. and Shastry, C. A. (1984) Present status of the geochronology of the Precambrian rocks of Rajasthan. Tectonophysics, v.105, pp.131-140.

Coney, P.J. (1980) Cordilleran metamorphic core complexes: An overview. Geol Soc. Amer. Mem., v.153, pp.7-31.

Deb, M., Thorpe, R.I., Krstic, D., Corfu, F. and Davis, D.W. (2001) Zircon U-Pb and galena Pb isotope evidence for an approximate 1.0 Ga terrane constituting the western margin of the Aravalli–Delhi orogenic belt, northwestern India. Precambrian Res., v.108, pp.195-213.

Dunlap, W. J., Hirth, G. and Teyssier, C. (1997) Thermo-mechanical evolution of a ductile duplex. Tectonics, v.16, pp.983-1000.

Eskola. P.E. (1949) The problem of mantled gneiss domes. Geol. Soc. London, Quart. Jour., v.104, pp.461-476.

Fareeduddin, Reddy, M. S. and Bose, U. (1995) Reappraisal of the Delhi stratigraphy in the Ajmer – Sambhar sector, north central Rajasthan. Jour. Geol. Soc. India, v.45, pp.667-679.

Fowler, A.R., Khamees, H. and Dowidar, H. (2007) El Sibai gneissic complex, Central Eastern Desert, Egypt: Folded nappes and syn-kinematic gneissic granitoid sheets – not a core complex. Jour. African Earth Sci., v.49, pp.119-135

Fowler, T.J. and Osman, A.F. (2001) Gneiss-cored interference dome associated with two phases of late Pan-African thrusting in the central Eastern Desert, Egypt. Precambrian Res., v.108, pp.7-43.

Fritz, H., Wallbrecher, E., Khudeir, A.A., Abu El Ela, F. and Dallmeyer, D.R. (1996) Formation of Neoproterozoic metamorphic core complexes during oblique convergence (Eastern Desert, Egypt). Jour. African Earth Sci., v.23, pp.311-329.

Gupta, P., Fareeduddin, Reddy, M.S. and Mukhopadhyay, K. (1995) Stratigraphy and structure of Delhi Supergroup of rocks in central part of Aravalli range. Rec. Geol. Surv. India, v.120, pp.12-26.

Harris, L.B., Koyi, H.A. and Fossen, H. (2002) Mchanisms for folding of high grade rocks in extensional tectonic settings. Earth Sci. Rev., v.59, pp.163-210.

Heron, A.M. (1953) The geology of Central Rajputana. Mem. Geol. Surv. India, v.79, 389p.

Kisters, A. F. M., Stevens, G., Dziggel, A. and Richard A. Armstrong (2003) Extensional detachment faulting and core-complex formation in the southern Barberton granite–greenstone terrain, South Africa: evidence for a 3.2 Ga orogenic collapse. Precambrian Res., v.127, pp.355–378.

Lister, G. S. and Davis, G.A. (1989) The origin of metamorphic core complexes and detachment faults formed during Tertiary continental extension in the northern Colorado River region, U.S.A. Jour. Struct. Geol., v.11, pp.65-94.

Lopez, R., Mukhopadhyay, D., Bhattacharya, T. and Tobisch, O. T. (1996) Proterozoic rim and core zircon ages from the Anasagar gneiss, central Rajasthan, India. Geol. Soc. Amer., Abstract and Programs, v.28(7), pp.A 492.

Makovsky, Y, Klemperer, S. I., Ratsbacher, L. and Alsdorf, D. (1999) Midcrustal reflector on INDEPTH wide-angle profiles: An ophiolitic slabbeneath the India-Asia suture in southern Tibet? Tectonics, v.18, pp.793-808.

Martinez-Martinez, J. M., Soto, J. I. and Balanya, J. C. (2002) Orthogonal folding of extensional detachments: structure and origin of the Sierra Nevada elongated dome (Betics, SE Spain). Tectonics, v.21, pp. 3-1-3-22.

Mukhopadhyay, D. (1989) Structural history of the central section of the Delhi orogenic belt. Proc. 28th. Int. Geol. Cong., Abstract, v.2, pp.2-479-2-480.

Mukhopadhyay, D. and Bhattacharyya, T. (2000) Tectono-stratigraphic framework of the South Delhi Fold Belt in the Ajmer-Beawar region, central Rajasthan, India: a critical review. *In:* M. Deb (Ed.), Crustal evolution and metallogeny in the northwestern Indian shield. Narosa Publishing, New Delhi, pp.126-137.

Mukhopadhyay, D., Baral, M.C. and Niyogi, R.K. (1997) Structures in the banded iron-formation of the south-eastern Bababudan Hills, Karnataka. India. Proc. Indian Acad. Sci. (Earth Planet. Sci.), v.106, pp.259-276.

Mukhopadhyay, D., Bhattacharya, T., Chattopadhyay, N., Lopez,

R. and Tobisch, O.T. (2000) Anasagar gneiss: A folded granitoid pluton in the Proterozoic South Delhi Fold Belt, central Rajasthan. Proc. Indian Acad. Sci. (Earth Planet. Sci.), v.109, pp.21- 37.

Ramberg, H. (1981) Gravity, deformation and the Earth's crust: In theory, experiments and geological application. Academic Press, New York, 452p.

Roy, A.B. and Jakhar, S.R. (2002) Geology of Rajasthan (Northwest India) Precambrian to recent. Scientific Publishers (India), Jodhpur. 421p.

Sinha Roy, S., Malhotra, G. and Mohanty, M. (1998) Geology of Rajasthan. Geol. Soc. India, 278p.

Teyssier, C. and Whitney, D.I. (2002) Gneiss domes and orogeny. Geology, v.30, pp.1139-1142.

Tobisch, O. T., Collerson, K. D., Bhattacharya, T. and Mukhopadhyay, D. (1994) Structural relationship and Sm-Nd isotope systematics of polymetamorphic granitic gneisses and granitic rocks from central Rajasthan, India: implications for the evolution of the Aravalli craton. Precambrian Res., v.65, pp.319-339.

Volpe, A.M. and Macdougall, J.D. (1990) Geochemistry and isotopic characteristic of mafic (Phulad ophiolite) and related rocks in the Delhi Supergroup, Rajasthan, India: Implicationsfor rifting in the proterozoic. Precambrian Res., v.48, pp.167-191.

Wernicke, B. and Axen, G.J. (1988) On the role of isostasy in the evolution of normal fault systems. Geology, v.16, pp.848-851.

Whitney, D.L., Teyssier, C. and Vanderhaege, O. (2004) Gneiss domes and crustal flow. Geol Soc. Amer., Spec. Paper, v.380, pp.15-33.

Woodcock, N.H. (1977) Specification of fabric shapes using an eigenvalues method. Geol. Soc. Amer. Bull., v.88, pp.1231-1236.

Yin, A. (1991) Mechanisms for the formation of domal and basinal detachment faults: a three-dimensional analysis. Jour. Geophys. Res., v.96, pp.14,577-14,594.

Yin, A. (2002) Passive-roof thrust model for the emplacement of the Pelona-Orocopia Schist in southern California, United States. Geology, v.30, pp.183-186.

Yin, A. (2004) Gneiss domes and gneiss dome systems. Geol. Soc. Amer., Spec. Paper, v.380, pp.1-14.

(Received: 13 January 2009; Revised form accepted: 12 March 2009)